Journal of Solid State Chemistry 266 (2018) 1–8

Contents lists available at ScienceDirect

Journal of Solid State Chemistry

journal homepage: www.elsevier.com/locate/jssc

Crystal structure and monoclinic distortion of glaserite-type $Ba_3MnSi_2O_8$

Maxim Avdeev[a,b,*], Qingbo Xia[a,b], Matthew Sale[a,b], Morgan Allison[b], Chris D. Ling[a,b]

[a] Australian Nuclear Science and Technology Organisation, New Illawarra Road, Lucas Heights, NSW 2234, Australia
[b] School of Chemistry, The University of Sydney, Sydney 2006, Australia

ARTICLE INFO

Keywords:
Crystal structure
Glaserite
Neutron diffraction
Phase transition

ABSTRACT

Crystal structure and magnetic properties of glaserite-type $Ba_3MnSi_2O_8$ were investigated using variable temperature neutron powder diffraction and magnetometry. At room temperature the composition is hexagonal and the crystal structure is best described by the *P*-3*m*1 space group (a~ 5.7 Å, c~ 7.3 Å) with the apical oxygen atom modelled on a split site. On cooling below ~ 250 K the structure undergoes a phase transition into a monoclinic *C*2/*c* form ($\sqrt{3}a_{hex}$, a_{hex}, $2c_{hex}$, β~ 90°). Analysing diffraction data in terms of symmetry-adapted distortion modes suggests that the transition is primarily driven by increasing in-plane displacements of O1, which in turn results in the coupled tilting of [SiO_4] and [MnO_6] octahedra and in-plane displacements of Ba1 atoms. Magnetic susceptibility measurements and neutron powder diffraction data show no evidence for long-range magnetic ordering down to 1.6 K, although the development of magnetic diffuse scattering suggests that a magnetic transition may take place at lower temperature.

1. Introduction

Light emitting diodes (LED) are steadily replacing incandescent light sources owing to their higher energy efficiency and longer lifetime. A large family of silicates with the general formula $A_3MSi_2O_8$ (A=Ca, Sr, Ba; M=Mg) has attracted substantial interest as phosphor materials for LEDs [1,2].. In particular, glaserite-type hexagonal $Ba_3MgSi_2O_8$ shows very high tunability of emission which depends on the type of activation ion (Eu^{2+}, Mn^{2+}, Tb^{3+}) or mixture thereof [3,4]. The incorporation of Mn^{2+} into the structure was assumed to occur on the Mg^{2+} site due to its similar ionic radius; however, the end member $Ba_3MnSi_2O_8$ was never investigated in detail. Although synthesis of $Ba_3MnSi_2O_8$ has been reported before, only the symmetry and unit cell dimensions were presented based on X-ray powder diffraction (XRPD) data [5]. The hexagonal symmetry and unit cell dimensions for $Ba_3MnSi_2O_8$ were reported to be very similar to those of $Ba_3MgSi_2O_8$ but the proposed space group was different: *P*6/*mmm* (#191) [5], rather than *P*-3*m*1(#164) [6–8] or *P*-3(#147) [9,10]. The lack of detailed crystal structural information motivated us to undertake a detailed crystal structural investigation of $Ba_3MnSi_2O_8$. Since the *P*-3 and *P*-3*m*1 models proposed for presumably isostructural $Ba_3MgSi_2O_8$ differ only subtly in the arrangement of oxygen atoms, we used neutron powder diffraction (NPD) which allows us to more accurately locate them in the presence of heavy elements than is possible with XRPD. In order to separate the dynamic and static oxygen disorder, discussed further in detail herein, NPD data were collected at low temperature. They revealed a structural phase transition, which we investigated further by variable temperature NPD. Additionally, the magnetic properties were probed by magnetometry and low-temperature NPD.

2. Experimental

The powder sample of $Ba_3MnSi_2O_8$ was prepared by a solid state reaction using $BaCO_3$ (99.98%, Aldrich), $MnCO_3$ (> 98.0%, B.D.H.) and SiO_2 (99.98%, Aldrich) as starting materials. The stoichiometric reactants were well mixed by ball milling with acetone at 360 rpm for 2 h. After drying at 80 °C, the homogenously milled mixture was sintered at 800 °C for 10 h to decompose the carbonates, following with an intermediate grinding. The final product $Ba_3MnSi_2O_8$ was obtained by undergoing a sintering process at 1200 °C for 20 h.

Progress of the synthesis was monitored by collecting XRPD data on Panalytical X'Pert Pro diffractometer. Sintering was repeated until XRPD data of the sample did not change between successive treatments. The XRPD pattern for the final product agreed very well with the data reported for $Ba_3MnSi_2O_8$ in the original paper [5] and showed presence of Ba_2SiO_4, a very common by-product in synthesis of similar silicates, e.g., $Ba_3MgSi_2O_8$ [6]. In the case of $Ba_3MnSi_2O_8$, formation of Ba_2SiO_4 also results from minute oxidation of Mn^{+2} into Mn_3O_4, which was found in the sample at the 1.4(1) wt% level.

Neutron powder diffraction (NPD) data were collected on the high-resolution powder diffractometer ECHIDNA at the OPAL research reactor (ANSTO, Lucas Heights, Australia). The sample was loaded in

* Corresponding author at: Australian Nuclear Science and Technology Organisation, New Illawarra Road, Lucas Heights, NSW 2234, Australia.
E-mail address: maxim.avdeev@ansto.gov.au (M. Avdeev).

https://doi.org/10.1016/j.jssc.2018.07.001
Received 24 May 2018; Received in revised form 27 June 2018; Accepted 2 July 2018
Available online 03 July 2018

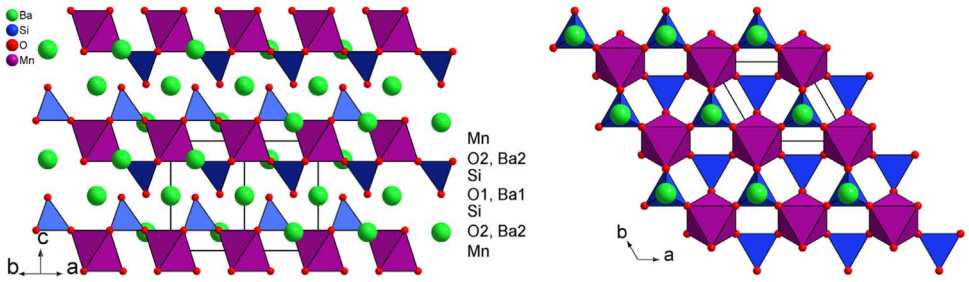

Fig. 1. Hexagonal structure of glaserite-type $Ba_3MnSi_2O_8$ along (110) (left) and (001) (right). Solid black lines outline the hexagonal unit cell with a~ 5.7 Å, c~ 7.3 Å.

powder form into a cylindrical vanadium can and NPD data were collected using a neutron wavelength of 1.6215 Å or 2.4395 Å in the temperature range from 1.6 K to 450 K. The Loopstra-Laar-Rietveld analysis [11,12] was performed using the GSAS suite of programs [13] with the EXPGUI front-end [14], and Fullprof [15]. Crystal structure and difference Fourier maps were visualized using the VESTA program [16].

The temperature-dependent magnetization of the samples was measured using a Quantum Design Physical Properties Measurement System (PPMS) with a vibrating sample magnetometer (VSM) probe from 2 to 300 K in an applied magnetic field 1 kOe, under zero field-cooled (ZFC) and field-cooled (FC) conditions.

3. Results and discussion

3.1. Room temperature neutron powder diffraction. Hexagonal structure

The glaserite crystal structure type has a general formula $XY_2[M(TO_4)_2]$ and is illustrated in Fig. 1. The structure can be viewed as one built of $[M(TO_4)_2]$ layers interleaved with X and Y cations. In the case of $Ba_3MnSi_2O_8$ X = Y = Ba and Ba1 and Ba2 atoms occupy two inequivalent sites 1b(0,0,1/2) and 2d(1/3,2/3,z), respectively (Fig. 1). Oxygen atoms of two types, O1 and O2, occupy two inequivalent sites 2d(1/3,2/3,z) and 6i(x,-*x*,z) coordinating Si with the ratio 1:3. The three equatorial O2 oxygen atoms of the silicate groups connect the three adjacent $[MnO_6]$ octahedra, while apical O1 atoms point to the interlayer space filled with Ba atoms. As the result, the O1 and O2 atoms are coordinated by $Si^{+4} + Ba1^{+2}$ and $Si^{+4} + Mn^{+2}$, respectively. O1 may be expected to be more labile due to longer and weaker Ba1–O1 bond, compared to Mn-O2. This is discussed in further detail below on the basis of our NPD results.

The Loopstra-Laar-Rietveld analysis [11,12] of the NPD data collected at room temperature revealed that a hexagonal model with space group *P*-3*m*1 (#146) and a~ 5.7 Å, c~ 7.3 Å indexed all the diffraction peaks of the main phase, yielding acceptable agreement with the experimental data. However, examination of the obtained structural parameters revealed that apical Si-O1 distance is noticeably shorter than equatorial Si-O2, and the isotropic displacement parameter of O1 is anomalously large - about three times higher than that of O2 (Model 1 in Table 1). Difference Fourier maps also clearly showed additional off-axis nuclear density (Model 1 in Table 2). The same observation was previously made for other hexagonal glaserite-type materials and ascribed to librational movement of tetrahedral groups, e.g., $K_3Na(SeO_4)_2$ [17,18], $K_3Na(MoO_4)_2$ [19], $K_3Na(RuO_4)_2$ and $Rb_3Na(RuO_4)_2$ [20].

The anomalously high isotropic thermal parameter of O1 and short Si-O1 distance were also observed for $Ba_3MgSi_2O_8$. Several different crystal structural models were proposed to describe the apparent in-plane displacement of O1 from the ideal fixed (x = 1/3,y = 2/3) position. Aitasalo et al. proposed a model with O1 in a site of lower symmetry 6i(x,-*x*,z) [6]. Iwata et al. proposed a model in which not only the O1 site but also O2 and Ba1 are split [7]. Based on NPD data, Park et al. proposed a superstructure described by the P-3 space group with oxygen displacements ordered in a (√3a,√3a,c) hexagonal supercell [9]. All three models were tested against our NPD data for $Ba_3MnSi_2O_8$ (models 4–6 in Tables 1, 2, respectively). In addition, we tested the ideal glaserite model with isotropic displacement parameters (model 1), anisotropic displacement parameters for O1 only (model 2), and all atoms modelled anisotropically (model 3). Finally, we also tested a model describing $[SiO_4]$ groups as rigid-body units in combination with the Translation-Libration-Screw (TLS) formalism [21] which has previously been successfully applied to polyanionic materials such as silicates [22] (model 7).

The results for the tested seven models are summarized in Tables 1, 2. When comparing the models, attention was paid not only to the R-factors indicating quality of the NPD data fit, but also to the residual nuclear scattering density in difference Fourier maps. From comparison of the tested models, several conclusions can be drawn.

Modelling O1 anisotropically (model 2) significantly improves agreement between the calculated and experimental NPD data. The fit quality is practically identical to that for the model with a split O1 site [6] using the same number of variables, cf. models 2 and 4 in Table 1. The resulting axially oblate ellipsoid of atomic displacements for O1 in model 2 also substantially reduces the residual nuclear scattering density in the unit cell compared to that for the isotropic model 1, although not as well as the model with a split O1 site: cf. values for models 1, 2 and 4 in Table 2.

Splitting of the O2 and Ba1 sites in addition to O1, following Iwata et al. [7], results in further improvement (model 5 in Tables 1, 2) but not as significant as modelling all atoms in the ideal glaserite anisotropically (model 3).

In contrast to $Ba_3MgSi_2O_8$ [9], our NPD data for $Ba_3MnSi_2O_8$ showed no evidence of supercell reflections. As the results, refinement using the (√3a,√3a,c) P-3 model of Park et al. produced improvements neither in R-factors nor residual density of the difference Fourier map, despite the substantially higher number of variables (Tables 1, 2).

Finally, model 7 with coupled translational and librational movement of the rigid $[SiO_4]$ group (with the four Si-O distances fixed to the value most commonly observed in silicates [23]) gave an inferior fit (Tables 1, 2). This suggests that the $[SiO_4]$ groups in $Ba_3MnSi_2O_8$, and most likely other glaserite-type materials, are not truly rigid bodies, the apical O1 oxygen atoms are more labile than O2, which results in local silicate group distortion.

Comparison of the seven models tested for $Ba_3MnSi_2O_8$ showed that the fully anisotropic model #3 produced the best agreement with our room temperature NPD data (Table 1). This is in agreement with the bulk of literature on crystal structure determination for glaserite-type oxides. However, we emphasize that such a model is clearly only an approximation as it cannot resolve the problem of the unphysically short Si-O1 distance. The natural step was to combine the split O1 model #4 with the fully anisotropic description of all the other atoms. Indeed, model #8 yielded not only the same refinement quality but also the lowest residual nuclear density (Tables 1, 2). We therefore conclude that this is the most adequate model of crystal structure of $Ba_3MnSi_2O_8$ and likely all the other hexagonal glaserite-type oxides in the hexagonal